I - 4 Nonlinear FEM Analysis of Steel Members under Very-Low-Cycle Loading

Disas. Prev. Res. Inst., Member, JSCE, Yeon-Soo PARK
Disas. Prev. Res. Inst., Member, JSCE, Satoshi IWAI
Disas. Prev. Res. Inst., Member, JSCE, Hiroyuki KAMEDA
Disas. Prev. Res. Inst., Member, JSCE, Taijiro NONAKA

1. Introduction The main objective of the numerical analysis presented herein is to simulate the hysteretic behavior of steel angles under very-low-cycle loading, especially the history and cumulative state of local strain at their critical parts. Very-low-cycle loading is meant to involve load repetitions of the order of a few to twenty cycles after undergoing inelastic buckling. The computer model is based on a three-dimensional, nonlinear analysis by using the finite element program (FEM), MSC/NASTRAN, which includes the effects of the material and geometric nonlinearities. All computer runs have been made on the FUJITSU M-1800/30 computer system of the Data Processing Center, Kyoto University. The analysis has been performed in conjunction with the experimental works[1,2] which jointly constitute major parts of a comprehensive study.

2. FEM modeling and loading A typical finite element model for the angle L-40x40x3 is shown in Fig. 1. The 4-noded quadrilateral isoparametric shell elements (QUAD4 elements) were used in modeling the tested angle specimen. The material property in this analysis has been assumed to be bilinearly etasto-plastic with kinematic hardening. The yield stress σ_y, Young's modulus E_s and Poisson's ratio ν were taken to be 349 N/mm^2, 2.06x10^5 N/mm^2 and 0.3, respectively. The slope E_t, in the strain hardening region, of the stress-strain curve was selected at 1% of E_s. The von Mises yield criterion was used. Both ends of the specimen were modeled as simply supported. Both end-supporting parts of the test specimen by holding the blocks[1] were modeled by using the 3-noded stiff shell elements and the stiff QUAD4 elements for providing rigid-body motion in the vicinity of ends. As for the degrees of freedom, only the in-plane rotation was constrained in all the nodes of the model. The analyzed models were subjected to cyclic enforced axial displacement, in the contraction side (L3CP[1] model), alternate side (A3CP[2] model) and elongation side (T3CP[2] model) with a constant amplitude 8% of the length l. The load was applied with small eccentricities, about 0.2-1.0 mm distant from the gravity center at each end in the Z-direction (Fig. 1), in order to produce a desired deflection mode as observed in the experiment, as shown in Fig. 2. The analysis was basically performed up to the number of cycles where outbreak and/or penetration of cracks through the thickness of the angle leg were observed in the experiment. The analysis for each model took about 3 hours of CPU time on the average.

3. Axial load-displacement relations A comparison is made in Figs. 3 and 4 for the dimensionless load-axial displacement curves from the analysis and experiment. Here the load P and relative displacement Δ are normalized by the yield load N_y and length l, respectively. The analytical

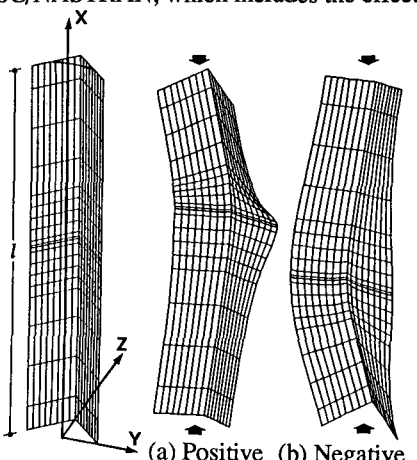

(a) Positive mode (b) Negative mode

Fig. 1 Typical model.

Fig. 2 Deformed shapes at Δ/l = -0.08.

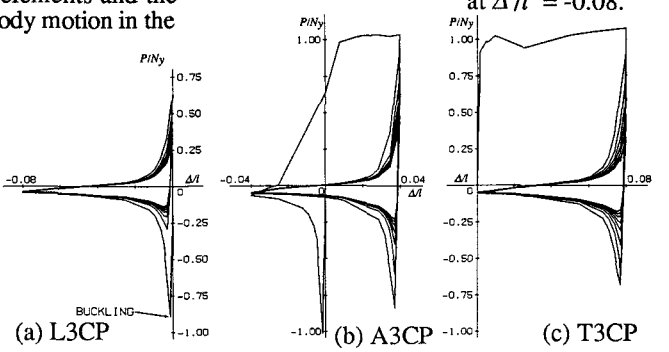

(a) L3CP (b) A3CP (c) T3CP

Fig. 3 Load-axial displacement relations [Analysis].

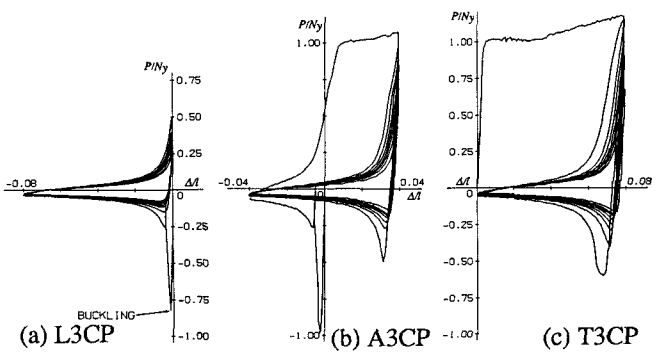

(a) L3CP (b) A3CP (c) T3CP

Fig. 4 Load-axial displacement relations [Experiment].

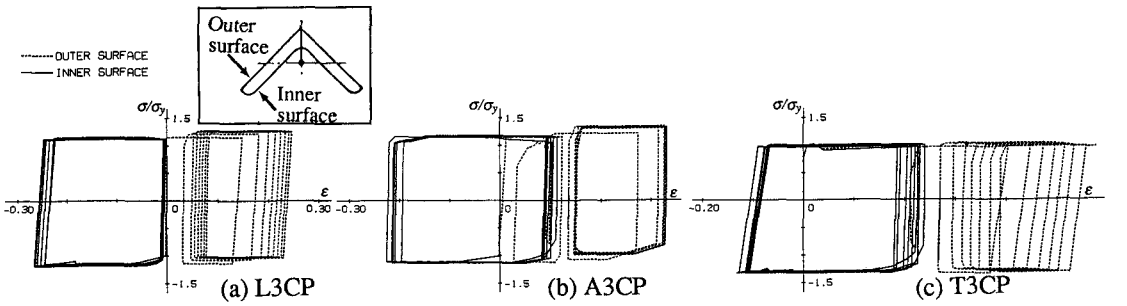

Fig. 5 Local stress-strain hysteresis [Analysis].

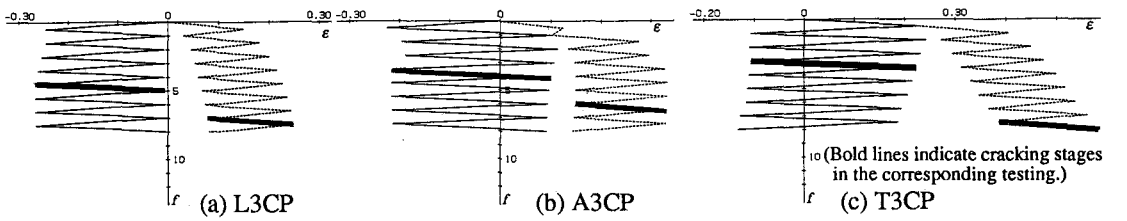

Fig. 6 Local strain histories with the increasing number of cycles [Analysis].

overall behaviors show good agreement with the experimental results. In the case of loading started from the contraction side (see (a) in Figs. 3 and 4), the compressive load decreased suddenly after the global buckling occurred at an early stage of the first cycle due to the inelastic local buckling. The compressive load-carrying capacities at each cycle after the first cycle were significantly deteriorated, but only a small decrease was seen in the succeeding tensile load-carrying capacities. Here one cycle is defined with reference to the load P=0, starting at zero, undergoing load reversal and returning to zero. The fairly higher compressive strength in the second cycle under the alternately constant displacement loading (A3CP model) was calculated by the numerical analysis, as indicated in Fig.3(b). This phenomenon may be attributed to the compressive loading for the nearly straight model regained by pure tensile yielding after being plastically deformed into a crooked configuration. In the case of loading started from a elongation side (Fig. 3(c)), the compressive strength in the first cycle was reduced considerably by the Bauschinger effect and the residual crookedness due to the eccentric tensile loading.

4. Tracing of local strain history Figs. 5 and 6 show the axial stress-strain hysteresis and the plastic local strain history, respectively, on the inner and outer surfaces of the edge element of the mid-height cross-section. The amplitudes of local strain on the inner surface of the critical elements were ranged approximately 10-40% in the first cycle. This indicate that the angle model under the very-low-cycle loading have partially experienced very large strain with inelastic local deformation. A small change of the amplitudes of plastic strain component per each cycle was observed such as a fatigue behavior. Regardless of the loading patterns, the strain amplitude on the inner surface is larger than that on the outer surface. Namely, the most severe concentration of local deformation occurs at the inner surface of the edge element of the mid-height portion. This seems to be the experimental phenomenon that the first cracking was observed on the concave side of the overall buckling deformation[1,2]. A trial computation was made for the summation of plastic components of strain in the tensile stress side in each cycle, up to the outbreaks of cracks indicated by bold lines in Fig. 6. This attained the values of 110-230%, irrespective of the loading patterns. These numbers correspond to the residual local strain of 90-120%[1,2] at the ruptured portion under the monotonic-tensile testing. This sum might be an indicator to represent the accumulated damage due to very low-cycle loading.

5. Concluding remarks The results of numerical analysis by the FEM program were presented for steel angle members under very low-cycles of loading. The overall behavior from the analysis shows good agreement with the experiment. The local strain history at the critical section was traced for large cyclic deformation by the numerical analysis. Under the very-low-cycles of loading, the angle model have partially experienced very large strain with inelastic local deformation. The most severe concentration of local deformation occurs on the concave surface of the overall buckling deformation.

References 1) S. Iwai, Y.-S. Park, T. Nonaka and H. Kameda: Very Low-Cycle Fatigue Tests of Steel Angle Members under Earthquake Loading, Proc. *10th World Conference on Earthquake Engineering*, Madrid, Vol. 5, pp. 2879-2884, 1992. 2) S. Iwai, Y.-S. Park, et al.: Tests on Very Low-Cycle Fatigue of Steel Members subjected to Reversed Displacement Loading, Proc. *Annual Conference of Kinki Branch of Architectural Institute of Japan,* 1993 (in Japanese).